New Journal of Physics
The open-access journal for physics

Optical nanoswitch: an engineered plasmonic nanoparticle with extreme parameters and giant anisotropy

Andrea Alù[1,2] **and Nader Engheta**[1]

[1] Department of Electrical and Systems Engineering, University of Pennsylvania, Philadelphia, PA 19104, USA
[2] Department of Electrical and Computer Engineering, University of Texas at Austin, Austin, TX 78712, USA
E-mail: andreaal@ee.upenn.edu and engheta@ee.upenn.edu

New Journal of Physics **11** (2009) 013026 (14pp)
Received 15 October 2008
Published 20 January 2009
Online at http://www.njp.org/
doi:10.1088/1367-2630/11/1/013026

Abstract. Naturally available optical materials are known to provide a wide variety of electric responses, spanning from positive to negative permittivity values. In contrast, owing to drastically modified conduction properties at the microscopic level, at such high frequencies magnetism and conductivity are very challenging to realize. This implies that extreme (high or low) values of permittivity, although highly desirable for a wide range of optical applications, are difficult to realize in practice. Here, we suggest the design of an engineered resonant nanoparticle composed of two conjoined hemispheres, whose optical response may be changed at will from an ideal electric conductor to an ideal magnetic conductor. Near the nanoparticle internal resonant frequency, we derive a closed-form solution that describes the electromagnetic response of this nanoparticle, showing how its light interaction may become dramatically dependent on the local field polarization, passing through all possible impedance values (from zero to infinity) by a simple mechanical or polarization rotation. Considering realistic frequency dispersion and loss in optical materials, we further show that these concepts may be applied to different geometries, with possibility for future experimental feasibility. We forecast various applications of this geometry as an optical nanoswitch, a novel nanocircuit element and as a building block for novel optical metamaterials.

Contents

1. Introduction

Light interaction with plasmonic materials gives rise to many anomalous optical phenomena based on localized plasmonic resonances, which have been the subject of studies over many decades [1]. One such striking effect consists of the superlensing properties of a plasmonic slab [2]: a planar layer with permittivity $-\varepsilon_0$, with ε_0 being the permittivity of free space, may lead to super-resolved images in the near field, due to the excitation of localized surface plasmons [3]. This effect may also be generalized to a pair of slabs with 'complementary' properties [4], i.e. oppositely signed permittivities and/or permeabilities, whose combined plasmon resonance, supported at their common interface, induces resonant tunneling and super-resolution.

Here, we analyze a different geometry that may exploit the localized resonance at the internal interface between the 'complementary' plasmonic and non-plasmonic materials in order to achieve a highly desirable, but conventionally difficult to realize [5], optical response. As depicted in figure 1, it consists of the combination of two conjoined hemispheres with oppositely signed permittivities. Around its internal resonant frequency, we derive in the following a quasi-static closed-form expression that shows how its optical response may become, for the same particle, both that of an ideal electric conductor and of an ideal magnetic conductor, depending on the orientation of the impinging electric field. This leads to giant anisotropy and the possibility of envisioning an optical nanoswitch that may shift its response from a perfectly electric to a perfectly magnetic conducting particle (i.e. from short to open circuit) at optical frequencies, despite lack of conductivity and magnetism in the involved materials at these frequencies [5]. This effect may pave the way to an exciting possibility for realizing extreme (high and low) tunable values of constitutive parameters at optical frequencies, for a variety of applications of interest, spanning optical communications [6], cloaking [7, 8] and optical nanocircuits [9]–[12].

2. Theoretical analysis

Consider the geometry of figure 1, i.e. a spherical nanoparticle of radius a, smaller than the wavelength of operation λ_0, composed of two conjoined hemispheres with different permittivities ε_{up} and $\varepsilon_{\text{down}}$, in a background with permittivity ε_0. The impinging electric field vector $\mathbf{E}_0$ is assumed to form a generic angle γ with respect to the z-axis. This problem does not

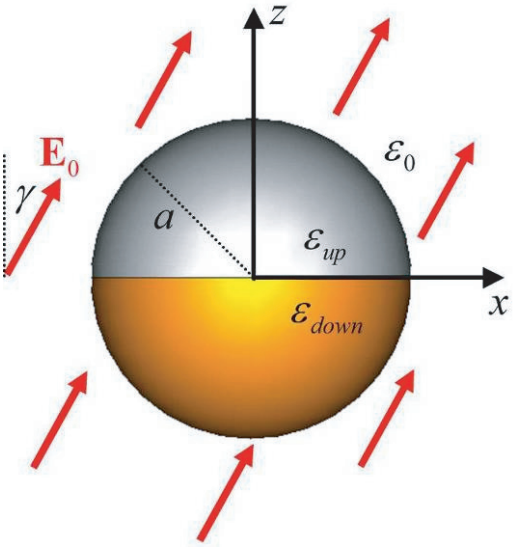

Figure 1. Geometry of the problem and reference system. Two conjoined spherical hemispheres are illuminated by a uniform electric field $\mathbf{E}_0$ lying in the xz-plane and forming an angle γ with the z-axis.

allow an analytical closed-form solution in the general case, but it may be solved with numerical methods.

Considering the mode-matching expansion in terms of spherical harmonics in each region of figure 1, the problem may be solved numerically in the small-radii limit, which is of interest here since $a \ll \lambda_0$, as suggested in [13]. In the most general case, the electric potential may be written in the different regions as

$$\begin{aligned}\phi_{\left\{\begin{smallmatrix}\text{up}\\ \text{down}\end{smallmatrix}\right.} &= E_0 \cos\gamma \sum_{n=0}^{\infty} h_n^{\left\{\begin{smallmatrix}\text{up}\\ \text{down}\end{smallmatrix}\right.} c_n \,(r/a)^n \, P_n\,(\cos\theta) \\ &\quad - E_0 \sin\gamma \sum_{n=0}^{\infty} h_{n+1}^{\left\{\begin{smallmatrix}\text{up}\\ \text{down}\end{smallmatrix}\right.} d_n \,(r/a)^n \, P_n^1\,(\cos\theta)\cos\varphi, \\ \phi_0 &= E_0 \cos\gamma \sum_{n=0}^{\infty} b_n \,(r/a)^{-n-1} \, P_n\,(\cos\theta) - E_0 \sin\gamma \sum_{n=0}^{\infty} f_n \,(r/a)^{-n-1} \, P_n^1\,(\cos\theta)\cos\varphi \\ &\quad - E_0 \cos\gamma \,(r/a)\, P_1\,(\cos\theta) + E_0 \sin\gamma \,(r/a)\, P_1^1\,(\cos\theta)\cos\varphi,\end{aligned} \tag{1}$$

where

$$h_n^{\text{up}} = \begin{cases} 1, & n \quad \text{even}, \\ \varepsilon_{\text{down}}/\varepsilon_{\text{up}}, & n \quad \text{odd} \end{cases}$$

and $h_n^{\text{down}} = 1$, which results from imposing the boundary conditions on the x–y-plane, and (r, θ, φ) are spherical coordinates referenced to the nanosphere center. The boundary conditions on the surface of the sphere allow obtaining the unknown sets of coefficients b_n, c_n, d_n and f_n. In particular, using the properties of the Legendre polynomials P_n and P_n^1, one can write the

following equations for b_n, c_n:

$$\sum_{n=0}^{\infty} b_n \left[(-1)^{n+l}(1+n+l\varepsilon_{\mathrm{rd}})+\eta_l(1+n+l\varepsilon_{\mathrm{ru}})\right] U_{nl} = -U_{1l}\left[(-1)^l(l\varepsilon_{\mathrm{rd}}-1)-\eta_l(l\varepsilon_{\mathrm{ru}}-1)\right],$$
$$\sum_{n=0}^{\infty} c_n \left[(-1)^{n+l}(1+l+n\varepsilon_{\mathrm{rd}})+\eta_n(1+l+n\varepsilon_{\mathrm{ru}})\right] U_{nl} = -U_{1l}\left[1-(-1)^l\right](l+2), \tag{2}$$

where $\varepsilon_{\mathrm{ru}} = \varepsilon_{\mathrm{up}}/\varepsilon_0$, $\varepsilon_{\mathrm{rd}} = \varepsilon_{\mathrm{down}}/\varepsilon_0$ and $U_{nl} = \int_0^1 P_n(x)P_l(x)\,\mathrm{d}x$, which may be evaluated in closed form [13]. An analogous pair of equations may be found for the coefficients f_n and d_n, obtainable from equations (2) after the substitutions $\eta_t \to \eta_{t+1}$ and $U_{nl} \to U^1_{nl} = \int_0^1 P^1_n(x)P^1_l(x)\,\mathrm{d}x$, respectively. By truncating the summation in each of these equations to a given order $N_{\max}$ and varying the order l from 0 to $N_{\max}$, four systems of equations are obtained, from which it is possible to solve numerically for the unknown coefficients. The convergence of these equations is generally assured, even if near the plasmonic resonances of the sphere (of which the internal one arises for the symmetric case when $\varepsilon_{\mathrm{up}} = -\varepsilon_{\mathrm{down}}$) the convergence may become extremely slow and only granted for sufficiently large n [14].

Consider now the ideal lossless situation in which $\varepsilon_{\mathrm{up}} = -\varepsilon_{\mathrm{down}}$, i.e. the spherical particle supports an internal plasmonic resonance (notice that this is totally independent of the value of the background permittivity ε_0). In this special case, the equations for b_n and f_n reduce to

$$\sum_{n=0}^{\infty} b_n \left[(1+n+l\varepsilon_{\mathrm{ru}})+(-1)^n(1+n-l\varepsilon_{\mathrm{ru}})\right] U_{nl} = 2l\varepsilon_{ru}U_{1l}, \tag{3}$$

$$\sum_{n=1}^{\infty} f_n \left[(1+n)(-1+(-1)^n)-l\varepsilon_{\mathrm{ru}}(1+(-1)^n)\right] U_{nl} = 2U_{1l}. \tag{4}$$

From equation (3), we can easily note that in this special case

$$b_1 = 1 \quad \text{and} \quad b_n = 0\ \forall n \neq 1. \tag{5}$$

Similar considerations apply to equation (4), implying

$$f_1 = -1/2 \quad \text{and} \quad f_n = 0\ \forall n \neq 1. \tag{6}$$

Since we are at the plasmonic resonance between the two hemispheres, it is not surprising that the systems for the internal coefficients c_n and d_n do not properly converge. The reason for this lack of convergence resides in the way in which equations (1) written, which assumes that no electric sources are present inside the nanoparticle. The plasmon resonance, on the other hand, weakens this condition, as it is confirmed by the fact that, when the possibility of having the term with $n = -1$ in the summations for ϕ_{up} and ϕ_{down} is assumed, the following extra conditions are obtained after applying similar considerations as above in solving the corresponding systems of equations:

$$c_{\pm 1} = \pm 1/\varepsilon_{\mathrm{ru}}, \quad d_1 = -1, \quad d_{-1} = -1/2, \quad c_n = d_n = 0\ \forall\ |n| \neq 1. \tag{7}$$

Despite the complexity of the boundary-value problem of figure 1, the simple conditions (5)–(7) provide a closed-form expression for the potential in the different regions, valid in the

limit $\varepsilon_{\text{up}} = -\varepsilon_{\text{down}}$:

$$\begin{aligned}\phi_0 &= E_0 \cos\gamma \left[(a/r)^2 - r/a\right] \cos\theta - E_0 \sin\gamma \left[\tfrac{1}{2}\,(r/a)^{-2} + r/a\right] \sin\theta \cos\varphi,\\ \phi_{\left\{\begin{smallmatrix}\text{up}\\ \text{down}\end{smallmatrix}\right.} &= E_0 \cos\gamma \left[(a/r)^2 - r/a\right] \cos\theta\, \varepsilon_0/\varepsilon_{\left\{\begin{smallmatrix}\text{up}\\ \text{down}\end{smallmatrix}\right.} - E_0 \sin\gamma \left[(a/r)^2/2 + r/a\right] \sin\theta \cos\varphi,\end{aligned} \tag{8}$$

where ϕ_0 is the potential distribution in the background region, ϕ_{up} and ϕ_{down} are the potentials in the upper and lower hemispheres, respectively.

3. Discussion

Equations (8) contain interesting information about the anomalous electromagnetic behavior of this resonant nanoparticle. We note that the total potential ϕ_0 in the background region does not depend on the specific values of $\varepsilon_{\text{up}} = -\varepsilon_{\text{down}}$ and it may be simply described by the superposition of two terms, obtained for $\gamma = 0$ ($\mathbf{E}_0$ orthogonal to the interface between the two hemispheres) and for $\gamma = \pi/2$ ($\mathbf{E}_0$ parallel to the interface), respectively. This resembles the closed-form solution that we have derived for different purposes in an analogous cylindrical geometry in [11], but now this is applied to a 3D resonant nanoparticle in spherical geometry. For the first term, the potential is identically the same (i.e. zero) all over the surface of the sphere, and the potential distribution is exactly equal to the one produced by a perfect electric conducting homogeneous sphere. Conversely, the second term corresponds to the potential distribution from a perfectly magnetic homogeneous sphere, even if the involved materials are far from being conducting, nor magnetic.

The potential inside the nanosphere, on the other hand, is effectively produced and sustained by two singular 'virtual sources', centered at the origin. The presence of these sub-wavelength singularities, which are effectively the image of the 'sources' of the impinging plane wave (more specifically the images of 'point sources' at infinity that generate the plane wave excitation), is the result of the super-focusing properties of surface plasmons, in some sense recalling analogous virtual singularities in the planar geometry [2]–[4].

Figure 2 shows the electric potential (top) and electric field distribution (bottom) in the x–z-plane for a nanosphere with $a = 10\,\text{nm}$, $\varepsilon_{\text{up}} = -16\,\varepsilon_0$, $\varepsilon_{\text{down}} = 16\,\varepsilon_0$, which may represent, respectively, silver and silicon, around 500 THz when neglecting losses (in the next section, we will also take into account the material absorption). In this scenario $\gamma = 0$ ($\mathbf{E}_0 \parallel \hat{\mathbf{z}}$) and the surface of the nanosphere is equipotential, with electric field all orthogonal to it, as predicted by equations (8). For an external observer, the nanoparticle behaves as a perfectly electric conducting particle, with extremely large effective permittivity, even though no conductive material is being employed at optical frequencies. Inside the nanoparticle, however, the field is nonzero and a strong circulation of resonant displacement current is supported by the two singular points (two negative charges for this geometry) located at the origin. The dual behavior for the internal field, i.e. the presence of two positive charges at the origin, may be obtained by flipping the particle by 180°, i.e. by having $\varepsilon_{\text{up}} = 16\,\varepsilon_0$, $\varepsilon_{\text{down}} = -16\,\varepsilon_0$. The field distribution is consistent with the series resonance between a nanoinductor (plasmonic hemisphere) and a nanocapacitor (dielectric hemisphere), as has been extensively discussed in [11] for the analogous 2D geometry, interpreting the problem in terms of nanocircuit theory [9]–[11]. Consistent with a resonant circuit, an observer outside the particle would simply experience the presence of a perfectly conducting object (i.e. short circuit), without possibly detecting the

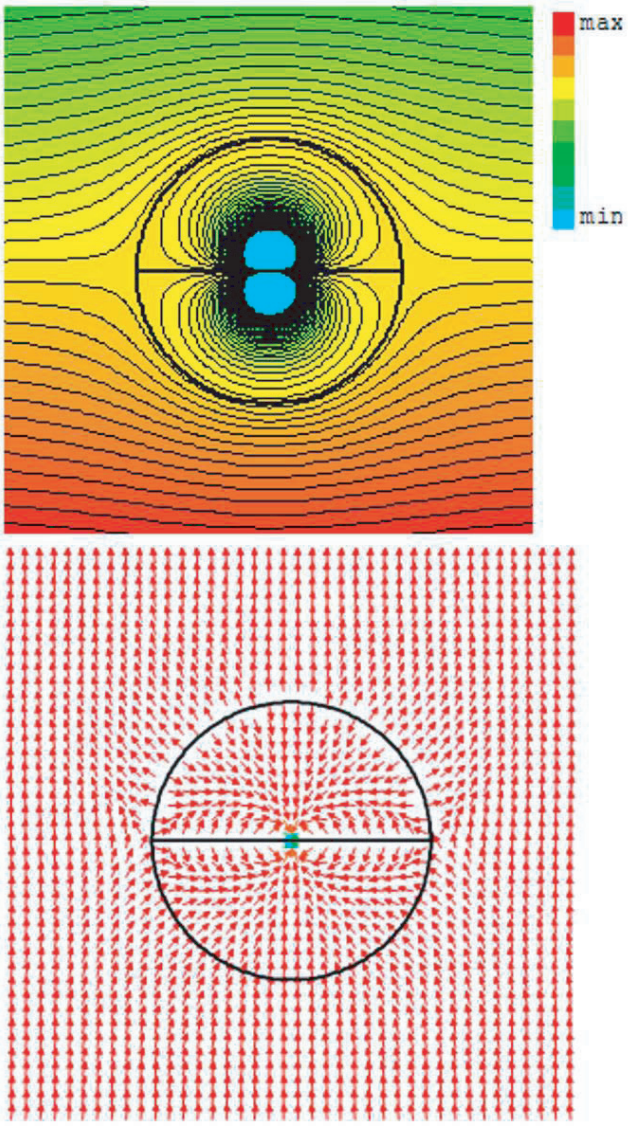

Figure 2. Orthogonal polarization: equivalence with a perfectly electric conducting sphere. Electric potential (top) and electric field distribution (bottom) on the x–z-plane for the geometry of figure 1 with $\varepsilon_{\mathrm{up}} = -16\varepsilon_0$, $\varepsilon_{\mathrm{down}} = 16\varepsilon_0$ and $\gamma = 0$. Darker (more red) colors correspond to larger potential values.

individual values of $\varepsilon_{\mathrm{up}}$ and $\varepsilon_{\mathrm{down}}$. However, the electric field inside the pair of hemispheres concentrates towards the singular point at the origin. Although the field is of infinitely high value (i.e. singular like) at the origin, and despite the presence of 'virtual' sources, it may be verified that the surface integral of flux $\boldsymbol{D}$ over any closed surface surrounding the origin is zero, proving that there is no real point charge at the origin and guaranteeing continuity of displacement current.

By simply rotating the electric field by 90°, the potential and electric field distributions are dramatically modified, as reported in figure 3. Now the equipotential lines are all orthogonal to the surface of the nanosphere and the electric field is tangential to it, exactly as if the

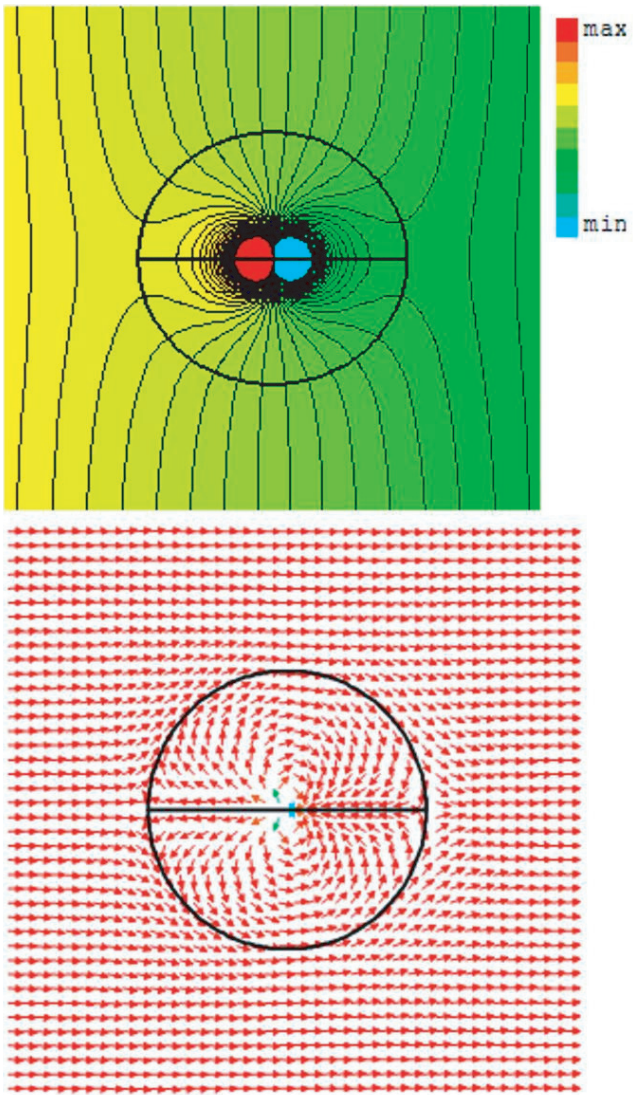

Figure 3. Parallel polarization: equivalence with a perfectly magnetic conducting sphere. Analogous to figure 2, but rotating the electric field to $\gamma = 90^{\circ}$.

nanoparticles were homogeneously filled by a perfectly magnetic conductor, with effective permittivity identically zero. Inside the nanoparticle the resonant field circulation is sustained by a virtual singular dipole at the origin, which is effectively the image of the 'sources' of the impinging plane wave focused at the center of the nanoparticle with infinite resolution (in this ideal situation in which losses are neglected). By duality, consistent with the discussion in [11] for the 2D geometry, this situation is completely consistent with the resonance of two nanoparticles interpreted as parallel combination of optical nanocircuit elements.

It is important to underline the giant anisotropy associated with this geometry, which allows this resonant spherical particle to act in its entirety as an optical 'nanoswitch', drastically changing its optical response from 'short circuit' (all the impinging displacement current flowing into and out of the sphere) to 'open circuit' (all the impinging displacement current avoiding entering the sphere), by the simple means of a mechanical rotation of 90°

(or corresponding rotation of polarization of the impinging electric field)[3]. This may have important applications in the framework of optical nanocircuits [9, 10].

As a special case, it is interesting to notice that the same potential and field distributions may be obtained with a simple hemisphere of permittivity $-\varepsilon_0$. In this special situation, the nanoparticle may enter into resonance with the surrounding 'complementary' hemisphere in the background, as a sort of hemispherical superlens with its focus at the origin, supporting an analogous effect of drastic dependence of its optical response on the orientation of $\mathbf{E}_0$.

The total electric field, evaluated as $\mathbf{E} = -\nabla\phi$ from equations (8), satisfies the following relations on the surface of the resonant nanosphere:

$$E_\theta/E_r|_{r=a} = \cos\varphi \tan\gamma/2, \;\; E_\varphi/E_r|_{r=a} = -\sin\varphi \tan\gamma/(2\cos\theta). \tag{9}$$

This confirms that the two limiting cases analyzed in figures 2 ($\gamma = 0$) and 3 ($\gamma = 90^\circ$) are characterized by normal and tangential electric fields with respect to the spherical surface, analogous to a perfect electric and a perfect magnetic homogeneous sphere, respectively. Equation (9) tells even more: it suggests that a rotation of the polarization of electric field (or of the particle) would gradually generate a tunable collection of 'intermediate' stages between a perfect electric and a perfect magnetic sphere, for which the angle between the electric field and the normal to the sphere is interestingly proportional to $\tan\gamma$. In some ways, the resonant sphere smoothly changes its optical response as 'seen' by the impinging field, varying the effective permittivity of the nanoparticle from 0 to ∞ as a function of the angle that the external electric field vector forms with its internal plasmonic interface. This phenomenon may be of extreme interest for a variety of optical applications, considering also the fact that such extreme values of constitutive parameters are challenging to realize naturally in practice, especially at these high frequencies [5, 6].

Figure 4 reports the cases of a hemisphere with $\varepsilon_{\text{up}} = -\varepsilon_0$ (left column), and the case with $\varepsilon_{\text{down}} = -\varepsilon_0$ (right) excited by a field with $\gamma = 45^\circ$. It is interesting to observe how the equipotential lines and the electric field vectors form, in the x–z-plane, a constant angle with the normal to the spherical surface in both cases (equal to the arctan $\frac{1}{2}$, following equation (9)), even in the hemispherical region where there is no permittivity contrast with the background. The potential distribution in the region $r > a$ is the same in the two cases, even if, to match the boundary conditions, the fields in the region $r < a$ are reversed from one case to the other. The image singularities at the origin are induced even in the region with $\varepsilon = \varepsilon_0$, associated with the supported plasmon resonance. For an external observer, the whole spherical surface in the x–z-plane looks homogeneous, and the impinging displacement current is divided into two parts; one flowing into and out of the sphere (related to E_r) and the other flowing to the outside (fringing) region (related to E_θ and E_ϕ). In particular, the ratio between the current flowing through the sphere and the one in the fringing field is locally determined, on the surface of the sphere, by the ratio between radial and tangential components of the electric field, as described in closed form in equation (9). This provides a novel form of field distribution on this spherical surface.

[3] Clearly, the conventional definition of a 'switch' would require the presence of some from of nonlinearity in the device, which would allow changing the state of the device from an 'ON' state to an 'OFF' state. Evidently, the nanoswitch presented here does not possess this kind of functionality, but instead we are referring here to the possibility of 'short circuiting' and 'open circuiting' the entire displacement current flow around the nanoparticle possibly by a means of a mechanical rotation of the particle. In this sense, the nanodevice indeed acts as a nanoswitch or a nanovalve in the framework of the optical nanocircuit paradigm [9, 10].

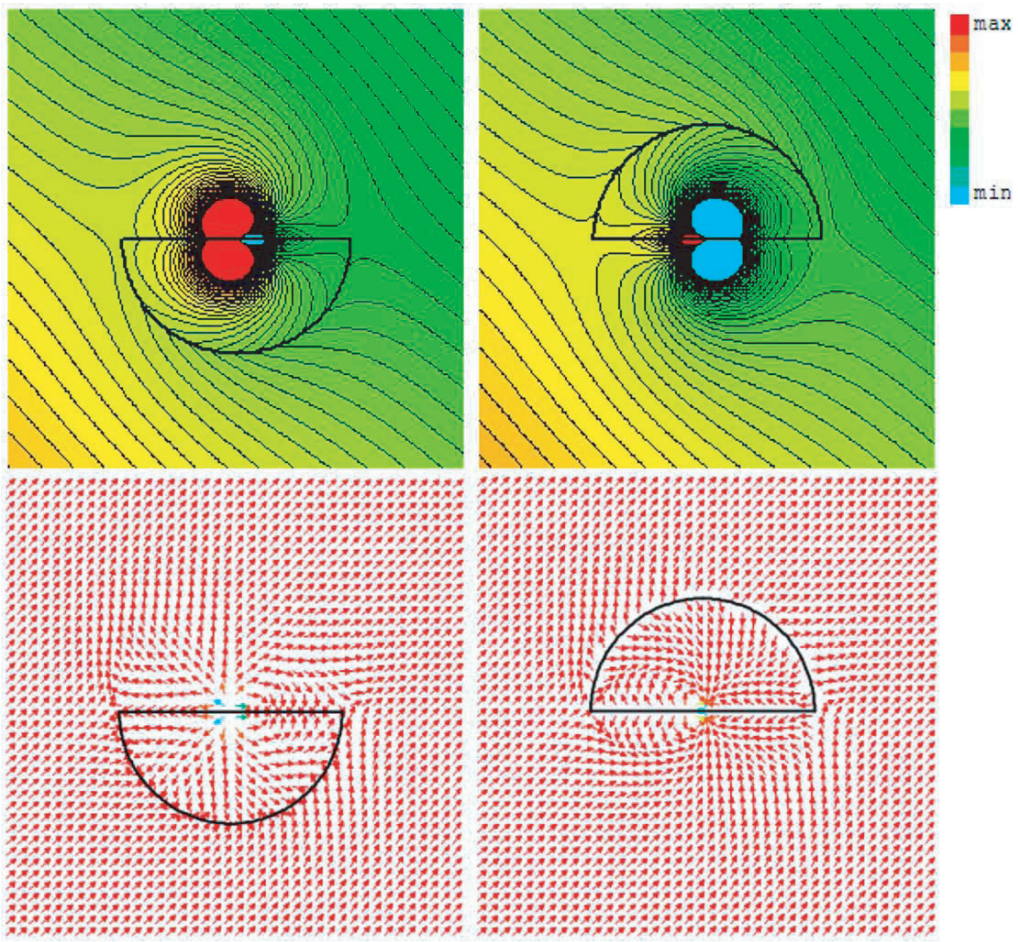

Figure 4. The special case of a resonant hemisphere: oblique polarization. Electric potential (top) and field distribution (bottom) on the x–z-plane for: (left) $\varepsilon_{\mathrm{up}} = -\varepsilon_{\mathrm{down}} = \varepsilon_0$ and (right) $\varepsilon_{\mathrm{up}} = -\varepsilon_{\mathrm{down}} = -\varepsilon_0$. In both cases $\gamma = 45^\circ$.

One notes how this ratio is drastically modified by simply varying the angle γ, consistent with the nanoswitch functionalities of this resonant plasmonic nanoparticle.

4. Towards the practical realization of a nanoswitch

In the previous sections, we have analyzed in detail the electromagnetic response of the nanoswitch in the ideal resonant situation $\varepsilon_{\mathrm{up}} = -\varepsilon_{\mathrm{down}}$, for which we have derived the closed-form solution (8) of the quasi-static electromagnetic problem. Although this analysis is very instructive and provides some useful insights into the anomalous response of this nanoparticle in this ideally resonant case, in practice it may be difficult to exactly realize such resonant condition, without using complex active inclusions. In any case, this condition may be achieved at one single frequency. More realistically, one has to deal with the general dispersion and presence of losses of the involved plasmonic materials.

The sensitivity of this resonance to losses and geometry imperfections may be modeled in terms of the optical nanocircuit theory [9]. In particular, the presence of absorption and

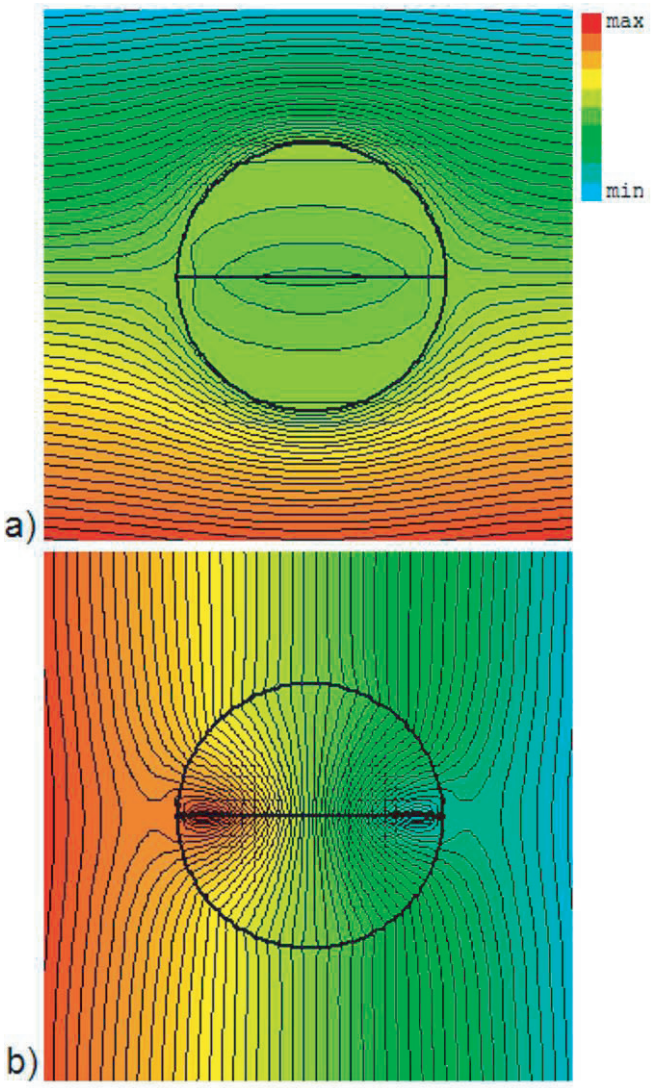

Figure 5. Robustness of the design: frequency mismatch and presence of losses. Electric potential distribution analogous to figure 2(a) ($\gamma = 0$, panel (a)) and figure 2(b) ($\gamma = \pi/2$, panel (b)), considering here realistic parameters for the materials, i.e. silicon and silver at the free-space wavelength $\lambda_0 = 600\,\text{nm}$.

imperfections in the involved materials is expected to lower the resonant Q of this system and smooth the singularities predicted by this lossless model. In figure 5, we have reported the numerical simulation, obtained using the mode-matching technique (1), for the electric potential distribution for the geometry of figures 2 and 3, but considering permittivity mismatch between the two materials and including realistic losses. In particular, in our numerical evaluation we have used $\varepsilon_{\text{up}} = (-16.05 + \text{i}\,0.44)\varepsilon_0$ and $\varepsilon_{\text{down}} = (15.89 + \text{i}\,0.103)\varepsilon_0$, which are the reported experimental values of permittivity for silver in [15] and silicon in [16] at the free-space wavelength of $\lambda_0 = 600\,\text{nm}$. It may be clearly seen that the concepts described here in the ideal (lossless) resonant limit are qualitatively preserved even when realistic losses and design variations are introduced. The singularities at the origin are now 'smoothed' and 'spread out'

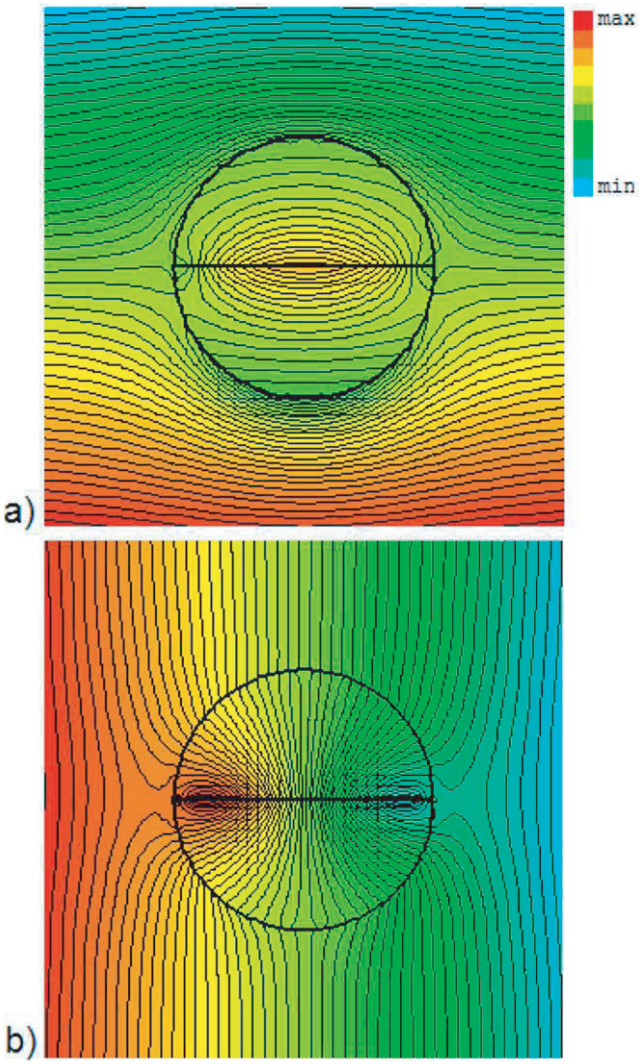

Figure 6. Silver and silicon nitride. Similar to figure 5, but using realistic parameters for silver and silicon nitride at $\lambda_0 = 400\,\text{nm}$.

all over the hemispheres' internal interface, due to these imperfections, but the giant anisotropy and extreme parameters of these nanoparticles are still very well preserved. This ensures that the extraordinary optical response of this resonant geometry is not limited to a single specific frequency of operation for which the closed-form solution (1) is valid, but rather it is also smoothly preserved over a certain bandwidth, which mainly depends, in this small-radii limit, on the permittivity dispersion of the involved plasmonic materials. These results also prove that the potential and field distributions indeed tend to the closed-form solution derived here (8) in the ideally resonant case.

As a second setup of interest that may lead to a future practical experimental verification of these concepts, in figure 6 we have reported the numerical simulation of a similar geometry, but using silver and silicon nitride at $\lambda_0 = 400\,\text{nm}$. In particular, $\varepsilon_{\text{up}} = 4.34\,\varepsilon_0$ [17] and $\varepsilon_{\text{down}} = (-4.35 + \text{i}\,0.21)\varepsilon_0$. In this scenario, we have also reversed the position of the silver hemisphere with respect to the impinging field as compared with figure 5, in order to verify the reversal of

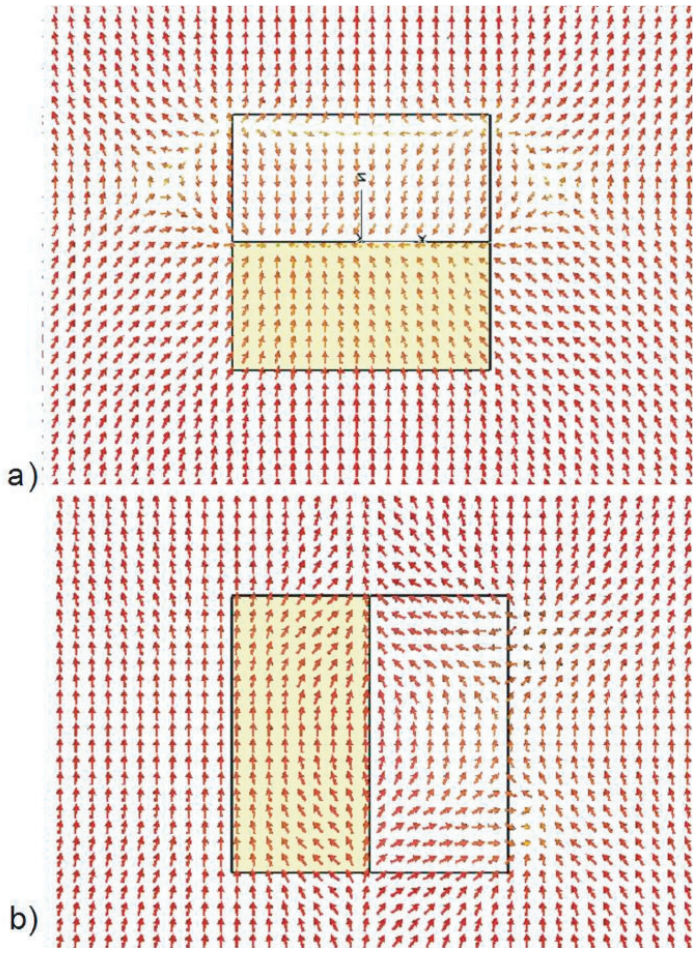

Figure 7. Resonant nanocube. Using the same materials and frequency as in figure 5, but considering now a cubic geometry, simulated using a full-wave simulation software package [18]. Snapshot in time of the electric field on the E-plane for a cube with side $l = 40$ nm. Panel (a) corresponds to the series excitation ($\gamma = 0$), whereas panel (b) corresponds to the parallel case ($\gamma = \pi/2$). The colored half-cube is made of the dielectric material.

polarization of the virtual sources in the series excitation (figure 5(a)). It is evident that in this setup the nanoswitch behavior is also very well preserved, despite the silver absorption and high frequency of operation.

Finally, in order to move another step towards a practical realization of these findings, we report in figures 7 and 8 the numerical simulations, obtained with full-wave finite difference software [18], for two cubic geometries formed by combining together two half-cubes made of the materials used in figures 5 and 6. Moreover, the wavelengths of operation are consistent with figures 5 and 6. In figure 7, the side of the cube is $l = 40$ nm, in figure 8, $l = 30$ nm, ensuring that in both simulations the nanocubes are subwavelength in size. It can be seen that even in this different geometry, at its internal resonance the cube becomes highly anisotropic and offers a behavior very similar to a perfectly electric conducting or a perfectly magnetic conducting cube, depending on the orientation of the external electric field. In particular,

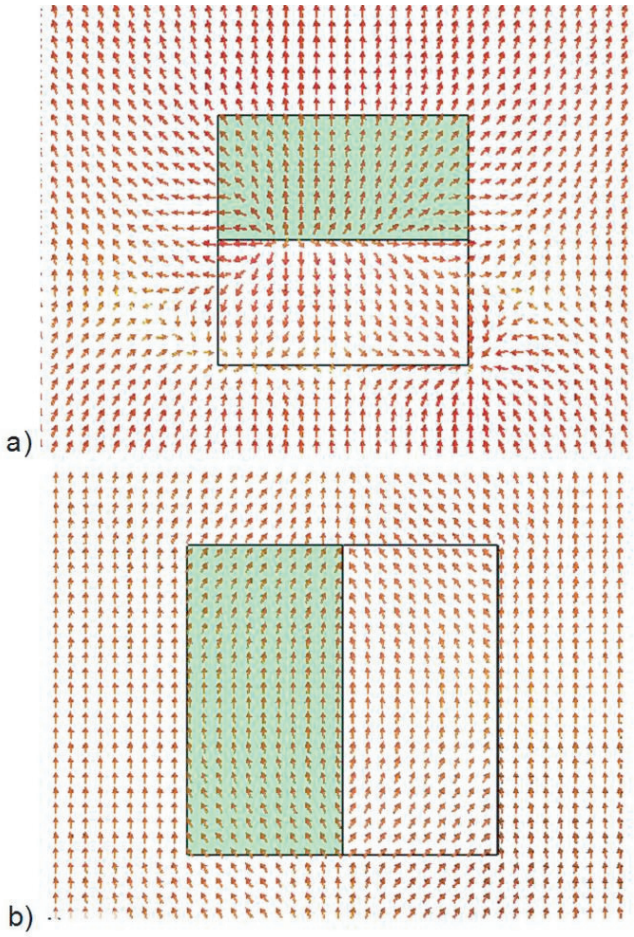

Figure 8. Silver and silicon nitride nanocube. Similar to figure 7, but for the set of materials and frequency of operation as in figure 6. In this case, $l = 30$ nm and also here the colored half-cube is made of the dielectric material.

despite the sharp resonances associated with the corners of the plasmonic half-cube and for the expected numerical noise associated with finite-difference time-domain numerical codes dealing with plasmonic interfaces [14, 19], it is indeed evident that the electric field tends to displace normal to the interfaces of the resonant cube in the series case and tangentially to it in the parallel situation (respectively, panels (a) and (b) in figures 7 and 8). These simulations fully take into account the realistic material losses and the frequency dispersion, as well as the dynamic nature of the field excitation. Indeed, they confirm that the quasi-static results reported in this paper are adequate and may be properly verified at optical frequencies using currently available materials and technology.

5. Conclusions

We have presented here the design of an engineered resonant nanoparticle whose optical response may be tuned at will from an ideal electric conductor to an ideal magnetic conductor. We have derived an elegant closed-form solution that describes its electromagnetic response in the quasi-static limit in the ideally resonant scenario, and we have confirmed these results with

full-wave simulations considering realistic frequency dispersion and loss in optical materials, as well as possible different geometries. Potential applications of these anomalous properties in tailoring the frequency response of optical nanocircuits [12] may be envisioned. Moreover, the possibility of realizing collections of these nanoparticles, effectively realizing perfect electric or magnetic metasurfaces and/or tunable optical nanomaterials is forecasted. Their response may be even tailored and tuned by the applied electric field polarization or by mechanically rotating the nanoparticles (e.g. using optical tweezers), at frequencies for which metal conductivity is usually absent or very low.

Acknowledgments

This work is supported in part by the US Air Force Office of Scientific Research (AFOSR) grant number FA9550-08-1-0220. We thank H Kettunen and A Sihvola for useful discussions on the mode-matching problem and M G Silveirinha for fruitful discussions.

References

[1] Kerker M 1991 Founding fathers of light scattering and surface-enhanced Raman scattering *Appl. Opt.* **30** 4699–705
[2] Pendry J B 2000 Negative refraction makes a perfect lens *Phys. Rev. Lett.* **85** 3966–99
[3] Taubner T, Korobkin D, Urzhumov Y, Shvets G and Hillenbrand R 2006 Near-field microscopy through a SiC superlens *Science* **313** 1595
[4] Alù A and Engheta N 2003 Pairing an epsilon-negative slab with a mu-negative slab: resonance, tunneling and transparency *IEEE Trans. Antennas Propag.* **51** 2558–71
[5] Landau L and Lifschitz E M 1984 *Electrodynamics of Continuous Media* (Oxford: Pergamon)
[6] Shen J T, Catrysse P B and Fan S 2005 Mechanism for designing metallic metamaterials with a high index of refraction *Phys. Rev. Lett.* **94** 197401
[7] Alù A and Engheta N 2005 Achieving transparency with plasmonic and metamaterial coatings *Phys. Rev.* E **72** 016623
[8] Pendry J B, Schurig D and Smith D R 2006 Controlling electromagnetic fields *Science* **312** 1780–2
[9] Engheta N, Salandrino A and Alù A 2005 Circuit elements at optical frequencies: nanoinductors, nanocapacitors and nanoresistors *Phys. Rev. Lett.* **95** 095504
[10] Engheta N 2007 Circuits with light at nanoscales: optical nanocircuits inspired by metamaterials *Science* **317** 1698–702
[11] Alù A, Salandrino A and Engheta N 2007 Parallel, series, and intermediate interconnections of optical nanocircuit elements—part 2: nanocircuit and physical interpretation *J. Opt. Soc. Am.* B **24** 3014–22
[12] Alù A, Young M and Engheta N 2008 Design of nanofilters for optical nanocircuits *Phys. Rev.* B **77** 144107
[13] Kettunen H, Wallén H and Sihvola A 2007 Polarizability of a dielectric hemisphere *J. Appl. Phys.* **102** 044105
[14] Kettunen H, Wallén H and Sihvola A 2008 Electrostatic resonances of a negative-permittivity hemisphere *J. Appl. Phys.* **103** 094112
[15] Jonhson P B and Christy R W 1972 Optical constants of the noble metals *Phys. Rev.* B **6** 4370
[16] Adachi S 1988 Model dielectric constants of Si and Ge *Phys. Rev.* B **38** 12966
[17] Djurisic A B and Li E H 1998 Modeling the index of refraction of insulating solids with a modified Lorentz oscillator model *Appl. Opt.* **37** 5291
[18] CST Design Studio 2008 http://www.cst.com.
[19] Zhao Y, Belov P and Hao Y 2007 Accurate modeling of the optical properties of left-handed media using a finite-difference time-domain method *Phys. Rev.* E **75** 037602